



## Utilization of sulfate additives in biomass combustion: fundamental and modeling aspects

**Wu, Hao; Jespersen, Jacob Boll; Grell, Morten Nedergaard; Aho, Martti; Jappe Frandsen, Flemming; Glarborg, Peter**

*Published in:*  
Proceedings of 21st European Biomass Conference and Exhibition

*Publication date:*  
2013

[Link back to DTU Orbit](#)

*Citation (APA):*  
Wu, H., Jespersen, J. B., Grell, M. N., Aho, M., Jappe Frandsen, F., & Glarborg, P. (2013). Utilization of sulfate additives in biomass combustion: fundamental and modeling aspects. In *Proceedings of 21st European Biomass Conference and Exhibition*

---

### General rights

Copyright and moral rights for the publications made accessible in the public portal are retained by the authors and/or other copyright owners and it is a condition of accessing publications that users recognise and abide by the legal requirements associated with these rights.

- Users may download and print one copy of any publication from the public portal for the purpose of private study or research.
- You may not further distribute the material or use it for any profit-making activity or commercial gain
- You may freely distribute the URL identifying the publication in the public portal

If you believe that this document breaches copyright please contact us providing details, and we will remove access to the work immediately and investigate your claim.

# Utilization of sulfate additives in biomass combustion: fundamental and modeling aspects

Hao Wu<sup>\*1</sup>, Jacob Boll Jespersen<sup>1</sup>, Morten Nedergaard<sup>1</sup>, Martti Aho<sup>2</sup>, Flemming Jappe Frandsen<sup>1</sup>, Peter Glarborg<sup>1</sup>

<sup>1</sup>Department of Chemical and Biochemical Engineering, Technical University of Denmark, Søtofts Plads, Building 229, DK-2800 Kgs. Lyngby, Denmark

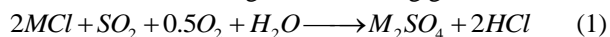
<sup>2</sup>VTT Technical Research Centre of Finland, P.O. Box 1603, FI-40101, Jyväskylä, Finland

## Abstract

Sulfates, such as ammonium sulfate, aluminum sulfate and ferric sulfate, are effective additives for converting the alkali chlorides released from biomass combustion to the less harmful alkali sulfates. Optimization of the use of these additives requires knowledge on their decomposition rate and product distribution under high temperature conditions. In the present work, the decomposition of ammonium sulfate, aluminum sulfate and ferric sulfate was studied respectively in a fast-heating rate thermogravimetric analyzer for deriving a kinetic model to describe the process. The yields of SO<sub>2</sub> and SO<sub>3</sub> from the decomposition were investigated experimentally in a tube reactor under different conditions, revealing that the ratio of the SO<sub>3</sub>/SO<sub>2</sub> released varied for different sulfate and the ratio could be influenced by the decomposition temperature. The proposed decomposition model of ferric sulfate was combined with a detailed gas-phase kinetic model of KCl sulfation and a model of K<sub>2</sub>SO<sub>4</sub> condensation to simulate the sulfation of KCl by ferric sulfate addition. The simulation results showed good agreements with the experiments conducted in a biomass grate-firing combustor, where ferric sulfate and elemental sulfur were used as additives. The results indicated that the SO<sub>3</sub> released from ferric sulfate decomposition was the main contributor to KCl sulfation and that the effectiveness of ferric sulfate addition was sensitive to the applied temperature conditions. Comparison of the effectiveness of different sulfates indicated that ammonium sulfate has clearly strongest sulfation power towards KCl at temperatures below 800°C, whereas the sulfation power of ferric and aluminum sulfates exceeds clearly that of ammonium sulfate between 900 and 1000°C. However, feeding gaseous SO<sub>3</sub> was found to be most effective to destroy KCl with a comparable dosage. Overall, the models developed in this work would facilitate an optimal use of sulfate additives in biomass combustion.

## Introduction

Alkali chlorides formed from the critical elements released from biomass combustion may lead to severe ash deposition and corrosion problems in biomass-fired boilers. One of the measures to reduce the alkali chloride-related problems in biomass combustion is to use additives to convert the alkali chloride to less harmful alkali species and release the chlorine as HCl [1]. Sulfur-based additives, such as elemental sulfur [2,3], SO<sub>2</sub> [3-6], ammonium sulfate [3,7-11], aluminum sulfate and ferric sulfate [6,12], have been tested in biomass combustion. Upon thermal decomposition or oxidation, these additives can produce SO<sub>2</sub> and SO<sub>3</sub>, which can convert the corrosive alkali chlorides to alkali sulfates and HCl through the following global reaction:



where *M* is K or Na.

The effectiveness of different sulfur-based additives has been investigated through experiments [2,3,5,6,12]. Sulfates, including ammonium sulfate, aluminum sulfate and ferric sulfate, are in general much more effective than elemental sulfur or SO<sub>2</sub> [2,3,6]. In a biomass-fired boiler where the gas residence time is typically only a few seconds, SO<sub>3</sub> is needed in order to achieve a fast sulfation of alkali chlorides [13]. However, the homogeneous oxidation of SO<sub>2</sub> to SO<sub>3</sub> is rather limited under boiler conditions as the reaction is thermodynamically restricted at high temperatures

(e.g. >1100°C), and kinetically limited at low temperatures (e.g. <900°C) [14,15]. Therefore, with the addition of SO<sub>2</sub> or elemental sulfur, only a small fraction would be oxidized to SO<sub>3</sub> and contribute to the sulfation reaction [2]. On the other hand, the thermal decomposition of sulfate additives is believed to produce SO<sub>3</sub> directly, resulting in a fast sulfation of alkali chlorides [2,12].

In spite of the extensive experimental studies on the utilization of sulfate additives [2,3,6,8,9,11,12,16], investigations on the decomposition rates and products of these additives are scarce. In relation to this, no modeling work has been carried out to simultaneously simulate the decomposition of the sulfate additives and the sulfation of potassium chloride under biomass-fired boiler conditions. The development of such a model would facilitate the optimization of sulfate additive utilization during biomass combustion.

## Specific objectives

The objectives of this study were to understand the decomposition behaviors of ammonium sulfate, aluminum sulfate and ferric sulfate under boiler conditions, and to develop a model to describe the sulfation of potassium chloride by sulfate addition during biomass combustion. A fast-heating rate thermogravimetric analyzer (TGA) and a tube reactor were used to study the decomposition kinetics and

\* Corresponding author: [haw@kt.dtu.dk](mailto:haw@kt.dtu.dk)

product distributions of the sulfates. The model developed in this work involved a description of sulfate decomposition, a detailed gas-phase kinetic model for sulfation of potassium chloride [14], and a simplified model for homogeneous and heterogeneous nucleation of potassium sulfate [17]. For validation of the model, the simulation results of ferric sulfate addition were compared with the results from biomass combustion experiments on a pilot-scale grate combustor, where ferric sulfate was injected in different amounts to the grate or into the freeboard [6]. In addition, a throughout comparison of the effectiveness of different sulfate was also conducted based on the simulation results.

## Experimental

Decomposition of ammonium sulfate, aluminum sulfate and ferric sulfate was studied respectively in a fast heating rate Netzsch STA 449 F1 Jupiter thermogravimetric analyzer (TGA). The experiments were carried out under  $N_2$  environment, using pure and dehydrated sulfates. During the TGA experiments, the dehydrated sulfate was heated at a rate of  $500^\circ\text{C}/\text{min}$  to an end temperature, and then it was kept at the temperature until a full-conversion was achieved. For different sulfate, different end temperatures were applied in the experiments. For the experiments of ammonium sulfate, the end temperatures were chosen to be in a range of  $200\text{--}350^\circ\text{C}$ . For the ferric sulfate experiments, the end temperatures were varied from  $600^\circ\text{C}$  to  $800^\circ\text{C}$ . For the aluminum sulfate experiments, the range of the end temperatures was  $700\text{--}800^\circ\text{C}$ .

In order to study the yields of  $SO_2$  and  $SO_3$  from the decomposition of ammonium sulfate, aluminum sulfate and ferric sulfate, experiments were conducted in a laboratory-scale tube reactor. The principles of the reactor and the experiments have been described in detail in our early work [18,19]. In the reactor, the decomposition of sulfate was carried out under well-defined temperature and flow conditions ( $5\text{ NL}/\text{min } N_2$ ), and the  $SO_2$  released were analyzed continuously by an IR-based gas analyzer. Based on the analyzed  $SO_2$  concentrations over time, a fractional conversion of the sulfur in ferric sulfate to  $SO_2$  at the given temperature condition was calculated. The remaining sulfur in ferric sulfate is assumed to be released as  $SO_3$ . The temperature range studied was  $500\text{--}1000^\circ\text{C}$ , where the conversion of  $SO_3$  to  $SO_2$  is expected to be negligible.

For validation of the model proposed in this work, the experiments conducted in a 100 kW grate combustor at the VTT Technical Research Centre of Finland, where ferric sulfate was tested as an additive to destruct alkali chlorides, were selected [6]. A schematic diagram of the grate combustor is shown in Figure 1. During the experiments, a mixture of Spanish wood chips and  $40\pm 4\%$  (energy basis) corn stover with compositions given in Table 1 was combusted on a rotating grate. The experiments were conducted at a constant fuel load of  $89\pm 5\text{ kW}$  which secured the temperature versus residence time profiles in the freeboard being representative of a grate-fired power plant [5]. The

temperatures in the freeboard were measured by a suction pyrometer at different sampling ports. At port Y5, an impactor was used to sample the alkali vapors and the small particulates generated from combustion. The chemical composition of the collected aerosols was analyzed by atomic absorption spectrometry (AAS) and ion chromatography (IC). The flue gas was analyzed by traditional on-line analyzers for  $O_2$ ,  $CO$  and  $CO_2$  after the cyclone placed downstream of the flue gas cooler. In addition, a flue gas flow was sampled at port Y7 to measure  $HCl$  and  $SO_2$  through a FTIR analyzer. For the experiments with ferric sulfate addition via port Y3, an aqueous solution of ferric sulfate was sprayed into the furnace with an average droplet size of  $\sim 12\text{ }\mu\text{m}$ . For the experiments with solid ferric sulfate or elemental sulfur addition to the grate, the additives were added to the fuel flow just before it enters to the grate. The dosage of sulfur additives, determined as the molar ratio of  $S_{\text{additive}}/Cl_{\text{fuel}}$ , was varied in the experiments.

GRATE COMBUSTOR (100 kW) – MEASURING AND SCALE SAMPLE POINTS

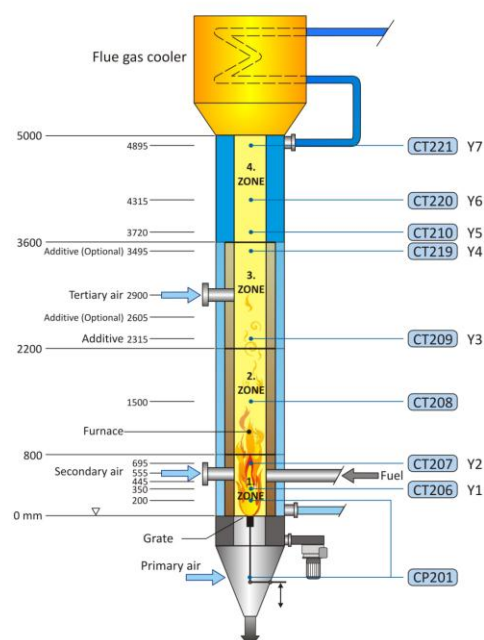


Figure 1. A schematic diagram of the 100 kW grate combustor at VTT Technical Research Centre of Finland [20].

Table 1 . Fuel analysis of a mixture of 60% wood chips and 40% corn stover.

Analysis	Unit	Value
Moisture	wt. %	29
LHV (as received)	MJ/kg	10.7
Ash	wt. % dry	8.0
S	wt. % dry	0.04
Cl	wt. % dry	0.305
C	wt. % dry	45.42
H	wt. % dry	5.69
N	wt. % dry	0.32
K	wt. % dry	0.83

### Model development

The model developed in this work involves a description of sulfate decomposition, a detailed reaction mechanism for the gas-phase reactions of  $\text{SO}_2/\text{SO}_3$  and  $\text{KCl}$  [13], and a simplified model for homogeneous condensation of  $\text{K}_2\text{SO}_4$  [16].

The decomposition of sulfate is assumed to be kinetically controlled and follow the volumetric reaction model:

$$\frac{dW}{dt} = -kW \quad (2)$$

where  $W$  is the relative mass of the anhydrous ferric sulfate defined as:

$$W = \frac{m - m_\infty}{m_0 - m_\infty} \quad (3)$$

where  $m_0$  (g) is the mass of the anhydrous sulfate before decomposition,  $m_\infty$  (g) is the mass of the residue after complete decomposition, and  $m$  (g) is the mass of anhydrous sulfate at  $t$  (s) during decomposition.

The rate constant  $k$  in Eq. 2 is assumed to follow an Arrhenius expression:

$$k = A \cdot \exp\left(-\frac{E}{RT}\right) \quad (4)$$

where  $A$  ( $\text{s}^{-1}$ ) is the pre-exponential factor,  $E$  (kJ/mol) the activation energy,  $R$  (kJ/mol/K) the gas constant, and  $T$  (K) the temperature of the particle. The activation energy ( $E$ ) and the pre-exponential factor ( $A$ ) in Eq. 4 are derived from the TGA experiments. As shown in Figure 2, during the isothermal periods of the fast-heating rate TGA experiments, a high linearity is generally seen between  $\ln(k)$  and  $1/T$ , indicating that Eq. 4 can satisfactorily describe the decomposition of the sulfates. Besides, it is also shown that the decomposition rate of sulfates studied in this work follows an order of ammonium sulfate > ferric sulfate > aluminum sulfate. The activation energy ( $E$ ) and the pre-exponential factor ( $A$ ) derived from Figure 2 for different sulfates are given in Table 2.

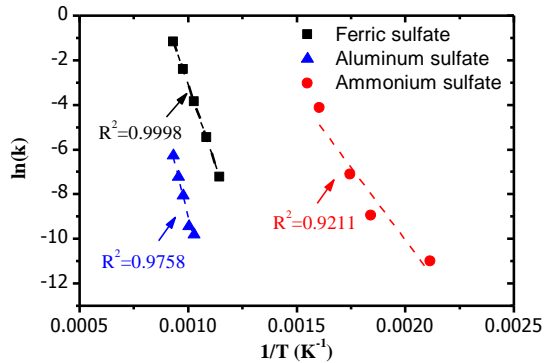


Figure 2. Correlation between  $\ln(k)$  and  $1/T$  during the decomposition of different sulfate in the TGA experiments under isothermal conditions.

Table 2 . Activation energy and pre-exponential factor derived from Figure 2.

	E/R (K)	A ( $\text{s}^{-1}$ )
Ammonium sulfate	13042	$9.15\text{E}+06$
Ferric sulfate	28480	$1.08\text{E}+11$
Aluminum sulfate	38782	$8.70\text{E}+12$

Figure 3 shows the results from the laboratory-scale tube reactor experiments. For ferric sulfate, it can be seen that approximately 60% of the sulfur in ferric sulfate is released as  $\text{SO}_2$  in the temperature range of 700–1000°C. Since the decomposition of ferric sulfate in a furnace primarily occurs at temperatures above 700°C, it is reasonable to assume for modeling purposes that 60% of the sulfur from ferric sulfate decomposition is released as  $\text{SO}_2$ , whereas the remaining 40% is released as  $\text{SO}_3$ . For aluminum sulfate, the yields of  $\text{SO}_2$  are much smaller than that of ferric sulfate, and the yields are not significantly influenced by decomposition temperature. Therefore, in the modeling, we assume that 15.8% (based on the average value of the measured data) of the sulfur of aluminum sulfate is released as  $\text{SO}_2$  and the remaining 84.2% is released as  $\text{SO}_3$ . For the decomposition of ammonium sulfate, the yields of  $\text{SO}_2$  increase almost linearly with increasing temperatures. Therefore, in the modeling, a linear correlation shown as in the dash line in Figure 3 is adopted to simulate the yields of  $\text{SO}_2$  from ammonium sulfate decomposition at different temperatures, and the remaining sulfur is assumed to be released as  $\text{SO}_3$ .

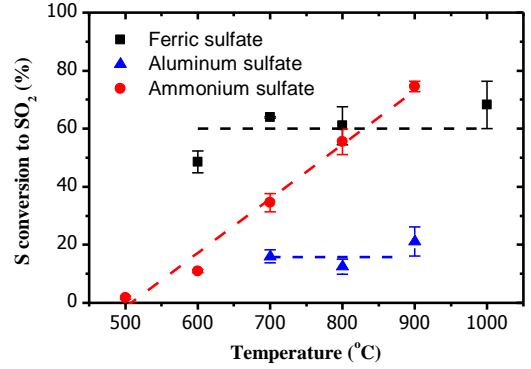


Figure 3. Yields of  $\text{SO}_2$  (%) during decomposition of sulfate under different temperatures, the remaining sulfur is assumed to be released as  $\text{SO}_3$ . The dash lines show the yields of  $\text{SO}_2$  used in the simulation.

In order to describe the gas phase reactions between potassium chloride and sulfur oxides released from ferric sulfate decomposition, the kinetic model proposed by Hindiyarti et al.[13] is adopted in this work. For homogeneous and heterogeneous condensation of potassium sulfate, a first order reaction as used by Li et al. [16] is chosen to describe the processes:



The rate constant for the reaction above, which represents the condensation rate predicted from aerosol theory [18], is:

$$k_{\text{condensation}} = 1 \times 10^{-61} \exp(-150000/T) \quad (6)$$

For the simulation of the experiments carried out at the VTT grate-reactor, the region of port Y1-Y7 of the reactor (see Figure 1) was modeled as an ideal plug flow reactor. The simulations were carried out with CHEMKIN 4.1.1, using the plug-flow reactor model. The temperature profile used in the simulation was pre-defined (see Figure 4), based on the averaged measured gas temperatures in the different experiments. The amount and composition of the inlet flue gas were estimated based on the experiment without ferric sulfate addition, where the fuel feeding rate was 0.0075 kg/s (wet basis) and the air feeding rate was 0.05 kg/s. The flue gas was assumed to contain only  $N_2$ ,  $O_2$ ,  $CO_2$ ,  $H_2O$ ,  $SO_2$ ,  $HCl$ , and  $KCl$ , with concentrations obtained from the gas analysis or aerosol measurement.

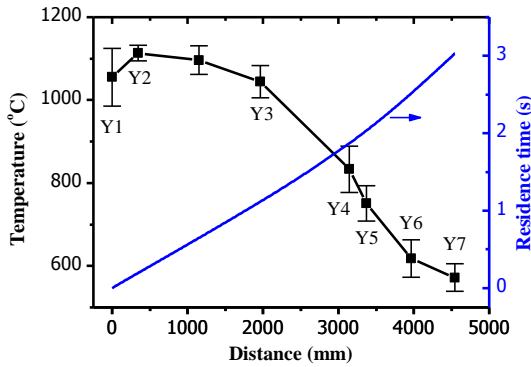


Figure 4. Temperature profile and residence time used in the simulation, from port Y1 to Y7 in Figure 1. The solid symbols represent the average temperatures measured in different experiments, with error bar showing the standard deviation.

For comparison of the effectiveness of the different sulfates and  $SO_3$ , simulations were carried out by using the plug-flow reactor model of CHEMKIN 4.1.1 at different temperatures, under a constant residence time of 1 s and a  $S_{additive}/KCl$  molar ratio of 1. The effectiveness was compared through a calculation of the degree of sulfation at the outlet of the reactor.

## Results and discussion

Figure 5 compares the measured and simulated  $SO_2$  emissions during the VTT grate-firing experiments. It can be seen that the emissions of  $SO_2$  are predicted well both for the experiments with elementary sulfur addition to the grate and for the experiments with ferric sulfate addition at port Y3 or to the grate.

In order to quantitatively describe the degree of sulfation during the VTT grate-firing experiments, the following parameter is introduced:

$$\text{Degree of sulfation} = 1 - \frac{Cl}{K + Na} \quad (7)$$

where the  $Cl$ ,  $K$  and  $Na$  are the relevant concentrations (mol%) in the aerosols collected at port Y5 of the reactor (see Figure 1).

The degree of sulfation described above is based on the assumption that the alkali metal found in the fine particles is comprised only of sulfates and chlorides. This assumption is believed to be reasonable for the

biomass mixture used in the VTT experiments, as the molar ratio of  $(K+Na)/(Cl+2S)$  is approximately 1 in the submicron aerosols collected from the experiments without additives. With the assumption, if all of alkalis in the aerosols are present as alkali chlorides, the calculated sulfation degree would be zero. On the other hand, if the aerosols only contain alkali sulfates, the calculated sulfation degree would be one. During the calculation of the sulfation degree in the experiments, particles in the size range of 0.03-0.62  $\mu m$  (in a few cases also the range of 0.03-0.26  $\mu m$ ) are considered in Eq. 9, because the majority of the alkali chlorides and sulfates are found in this size range [5]. Therefore it is believed that the sulfation degree calculated from the aerosols in this range is representative. In the simulation, the degree of sulfation is calculated by assuming that all of the  $KCl$ ,  $K_2Cl_2$ ,  $K_2SO_4$  and  $KHSO_4$  found at port Y5 will end up as aerosols. Therefore the relative concentrations of these species in the flue gas at port Y5 are used to calculate the sulfation degree in the simulation. Sodium is neglected in the simulation due to its small content in the fuel.

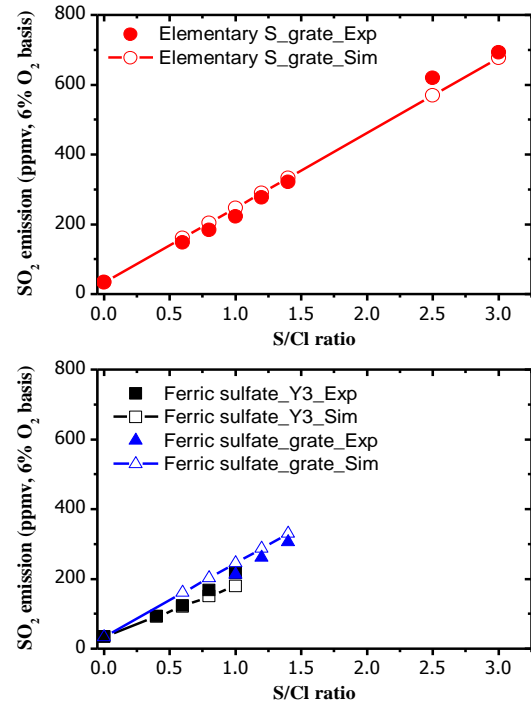


Figure 5 Simulated and measured  $SO_2$  emissions (ppmv, 6%  $O_2$  basis) in the dry flue gas of the VTT grate-firing experiments under different conditions.

The experimental and simulated degrees of sulfation during the VTT grate-firing experiments are shown in Figure 6. For the experiments with elementary sulfur addition, the experimental and simulation results are in good agreement, although the sulfation degree is slightly over-predicted by the simulation. For the experiments with ferric sulfation addition at port Y3, the simulation results compare favorably with the experimental results. However, for the experiments with ferric sulfate addition to the grate, the simulation appears to over-predict the sulfation degree considerably. A possible explanation is that the



simulation only considers the region from port Y1 to port Y7. The high-temperature region from the grate to port Y1 is neglected in the simulation, which may underestimate the conversion from  $\text{SO}_3$  to  $\text{SO}_2$ , thus resulting in an over-prediction of sulfation degree. The experimental and simulation results shown in Figure 6 imply that ferric sulfate is highly effective when it is injected to the post-combustion region via port Y3. However, when the ferric sulfate is added to the grate, its effectiveness on sulfation of alkali chlorides is almost as low as that of elementary sulfur.

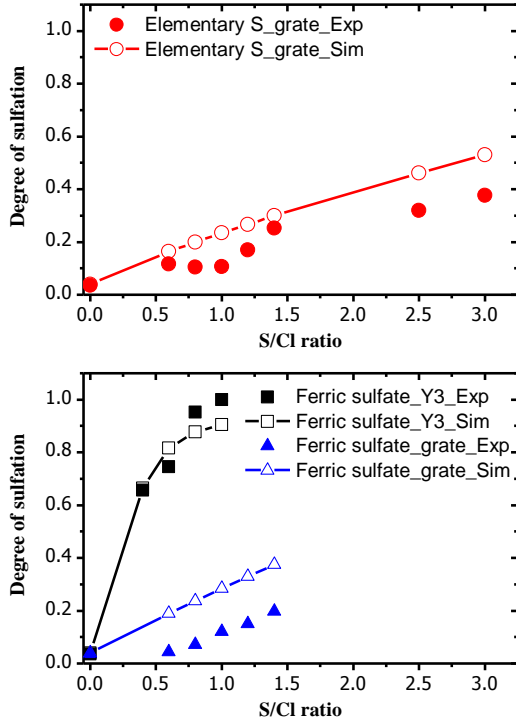


Figure 6 Simulated and measured degree of sulfation at port Y5 during the VTT grate-firing experiments.

Overall, the results of Figure 5 and Figure 6 suggest that the model developed for ferric sulfate can well simulate the experimental results. Since the experimental approaches are almost the identical for the other two sulfates (aluminum sulfate and ammonium sulfate), we believe that the model of other two sulfates would also well-predict the experimental results. However, validation of the model of these two sulfates is not considered in the scope of this work.

The effectiveness of different sulfates and  $\text{SO}_3$  under boiler conditions is compared through simulation. The results are shown in Figure 7. In this figure, the degree of sulfation is defined as:

$$\text{Degree of sulfation} = \frac{2 * ([K_2SO_4] + [KHSO_4])}{[KCl\_in]} \quad (8)$$

where  $[K_2SO_4]$  and  $[KHSO_4]$  are the concentrations of  $K_2SO_4$  and  $KHSO_4$  at the outlet of the reactor. Here, the concentration of  $KHSO_4$  is multiplied by a factor of 2, because one mole of  $KHSO_4$  would quickly capture one mole of  $KCl$  to form  $K_2SO_4$  and  $HCl$  when the temperature is decreased from the reactor temperature to atmosphere temperatures. However, the degree of

sulfation defined above may give a value that is greater than 1. Under these situations, the degree of sulfation is manually put to 1 in order to comply the physical meaning of the definition.

It can be seen from Figure 7 that ammonium sulfate is very effective, almost equal to  $\text{SO}_3$ , in the temperature range of 600-800 °C. This is primarily because that the decomposition of ammonium sulfate is sufficiently fast in this temperature range, and most of the sulfur (>50% as shown in Figure 3) is released as  $\text{SO}_3$  which can react with  $KCl$  rapidly. The effectiveness of ferric sulfate and aluminum sulfate is generally very low in the range of 600-800 °C, primarily due to the low decomposition rate of these two sulfates. In the temperature range of 800-1100 °C, the effectiveness of ammonium sulfate decreases with increasing temperatures. This is partly due to that more  $\text{SO}_2$  is released from ammonium sulfate decomposition when the temperature is increased (see Figure 3), resulting in a slower sulfation rate. On the other hand, even when  $\text{SO}_3$  is injected directly, its effectiveness still decreases with increasing temperature in the range of 800-1100 °C, as the formation of sulfates becomes thermodynamically restricted at high temperatures. For ferric sulfate and aluminum sulfate, a maximum  $KCl$  conversion is observed in the temperature of 900-1000 °C. This maximum conversion is related to a complete decomposition of these sulfates. However, when the temperature is increased further, even if the decomposition of sulfates is completed earlier, the effectiveness is still decreased as more  $\text{SO}_3$  will be converted to  $\text{SO}_2$  and the formation of sulfates becomes less thermodynamically favorable.

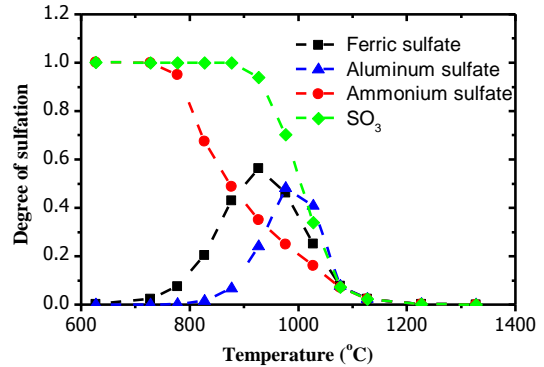


Figure 7 Comparison of the effectiveness of different sulfates and  $\text{SO}_3$  at different temperatures. The residence of in the reactor is 1 s and, the inlet  $KCl$  concentration is 29 ppmv, and the molar ratio of  $S_{\text{additive}}/KCl$  is 1.

Based on the results of Figure 7, one can conclude that ammonium sulfate has clearly strongest sulfation power towards  $KCl$  at temperatures below 800 °C, whereas the sulfation power of ferric and aluminum sulfates exceeds clearly that of ammonium sulfate between 900 and 1000 °C. However, feeding  $\text{SO}_3$  as gas is found to be most effective to destroy  $KCl$  with a comparable dosage. With known reaction conditions, the models developed in this work can be helpful in the selection and optimization of the use of additives.

## Conclusions

The decomposition rate of sulfates studied in this work followed an order of ammonium sulfate>ferric sulfate>aluminum sulfate. For the decomposition of ferric sulfate and aluminum sulfate, the yields of  $\text{SO}_3$  seemed to be independent of the decomposition temperature, with ferric sulfate constantly producing about 40%  $\text{SO}_3$  and aluminum sulfate generating about 84%  $\text{SO}_3$ . For ammonium sulfate, the yields of  $\text{SO}_3$  appeared to decrease with increasing decomposition temperature. The model developed for ferric sulfate simulated the experimental results obtained in a biomass grate-firing reactor well. The simulation results suggested that the  $\text{SO}_3$  released from ferric sulfate decomposition was the main contributor for KCl sulfation, and the effect of ferric sulfate addition on KCl destruction was sensitive to the applied temperature range. Comparison of the effectiveness of different sulfates indicated that ammonium sulfate has clearly strongest sulfation power towards KCl at temperatures below  $800^\circ\text{C}$ , whereas the sulfation power of ferric and aluminum sulfates exceeds clearly that of ammonium sulfate between  $900$  and  $1000^\circ\text{C}$ . However, feeding  $\text{SO}_3$  as gas was found to be most effective to destroy KCl with a comparable dosage.

## Acknowledgements

The Funding from EU contract 23946 “Demonstration of a 16 MW high energy efficient corn stover biomass power plant” was gratefully acknowledged.

## References

- [1] H. Wu, P. Glarborg, F.J. Frandsen, K. Dam-Johansen, P.A. Jensen, Dust-firing of straw and additives: ash chemistry and deposition behavior, *Energy Fuels*. 25 (2011) 2862-2873.
- [2] H. Kassman, L. Båfver, L.E. Åmand, The importance of  $\text{SO}_2$  and  $\text{SO}_3$  for sulphation of gaseous KCl-An experimental investigation in a biomass fired CFB boiler, *Combust. Flame*. 157 (2010) 1649-1657.
- [3] K.O. Davidsson, L.E. Åmand, B.M. Steenari, A.L. Elled, D. Eskilsson, B. Leckner, Countermeasures against alkali-related problems during combustion of biomass in a circulating fluidized bed boiler, *Chemical Engineering Science*. 63 (2008) 5314-5329.
- [4] Y. Zheng, P.A. Jensen, A.D. Jensen, B. Sander, H. Junker, Ash transformation during co-firing coal and straw, *Fuel*. 86 (2007) 1008-1020.
- [5] K. Iisa, Y. Lu, K. Salmenoja, Sulfation of potassium chloride at combustion conditions, *Energy Fuels*. 13 (1999) 1184-1190.
- [6] M. Aho, K. Paakkinen, R. Taipale, Destruction of alkali chlorides using sulphur and ferric sulphate during grate combustion of corn stover and wood chip blends, *Fuel*. 103 (2013) 562-569.
- [7] H. Wu, P. Glarborg, F.J. Frandsen, K. Dam-Johansen, P.A. Jensen, B. Sander, Trace elements in co-combustion of solid recovered fuel and coal, *Fuel Process. Technol.* 105 (2013) 212-221.
- [8] H. Kassman, M. Broström, M. Berg, L.E. Åmand, Measures to reduce chlorine in deposits: Application in a large-scale circulating fluidised bed boiler firing biomass, *Fuel*. 90 (2011) 1325-1334.
- [9] J.H. Zeuthen, P.A. Jensen, J.P. Jensen, H. Livbjerg, Aerosol formation during the combustion of straw with addition of sorbents, *Energy Fuels*. 21 (2007) 699-709.
- [10] H. Wu, P. Glarborg, F.J. Frandsen, K. Dam-Johansen, P.A. Jensen, B. Sander, Co-combustion of pulverized coal and solid recovered fuel in an entrained flow reactor – General combustion and ash behaviour, *Fuel*. 90 (2011) 1980-1991.
- [11] M. Broström, H. Kassman, A. Helgesson, M. Berg, C. Andersson, R. Backman, A. Nordin, Sulfation of corrosive alkali chlorides by ammonium sulfate in a biomass fired CFB boiler, *Fuel Process. Technol.* 88 (2007) 1171-1177.
- [12] M. Aho, P. Vainikka, R. Taipale, P. Yrjas, Effective new chemicals to prevent corrosion due to chlorine in power plant superheaters, *Fuel*. 87 (2008) 647-654.
- [13] P. Glarborg, P. Marshall, Mechanism and modeling of the formation of gaseous alkali sulfates, *Combust. Flame*. 141 (2005) 22-39.
- [14] L. Hindiyarti, F. Frandsen, H. Livbjerg, P. Glarborg, P. Marshall, An exploratory study of alkali sulfate aerosol formation during biomass combustion, *Fuel*. 87 (2008) 1591-1600.
- [15] T.L. Jørgensen, H. Livbjerg, P. Glarborg, Homogeneous and heterogeneously catalyzed oxidation of  $\text{SO}_2$ , *Chem. Eng. Sci.* 62 (2007) 4496-4499.
- [16] H. Kassman, J. Pettersson, B.M. Steenari, L.E. Åmand, Two strategies to reduce gaseous KCl and chlorine in deposits during biomass combustion— injection of ammonium sulphate and co-combustion with peat, *Fuel Process Technol.* (2011).
- [17] B. Li, Z. Sun, Z. Li, M. Aldén, J.G. Jakobsen, S. Hansen, P. Glarborg, Post-flame gas-phase sulfation of potassium chloride, *Combust. Flame*. 160 (2013) 959-969.
- [18] H. Wu, M. Castro, P.A. Jensen, F.J. Frandsen, P. Glarborg, K. Dam-Johansen, M. Røkke, K. Lundtorp, Release and transformation of inorganic elements in combustion of a high-phosphorus fuel, *Energy Fuels*. (2011) 2886.
- [19] A.R. Nielsen, M.B. Larsen, P. Glarborg, K. Dam-Johansen, High temperature release of  $\text{SO}_2$  from calcined cement raw materials, *Energy Fuels*. (2011).
- [20] M. Aho, K. Paakkinen, R. Taipale, Quality of deposits during grate combustion of corn stover and wood chip blends, *Fuel*. 104 (2013) 476-487.